Arch Appl Mech (2011) 81: 513–530
DOI 10.1007/s00419-010-0425-8

ORIGINAL

I. S. Shivakumara · S. Sureshkumar · N. Devaraju

Coriolis effect on thermal convection in a couple-stress fluid-saturated rotating rigid porous layer

Received: 16 July 2009 / Accepted: 19 March 2010 / Published online: 7 April 2010

Abstract Both linear and weakly nonlinear stability analyses are performed to study thermal convection in a rotating couple-stress fluid-saturated *rigid* porous layer. In the case of linear stability analysis, conditions for the occurrence of possible bifurcations are obtained. It is shown that Hopf bifurcation is possible due to Coriolis force, and it occurs at a lower value of the Rayleigh number at which the simple bifurcation occurs. In contrast to the nonrotating case, it is found that the couple-stress parameter plays a dual role in deciding the stability characteristics of the system, depending on the strength of rotation. Nonlinear stability analysis is carried out by constructing a set of coupled nonlinear ordinary differential equations using truncated representation of Fourier series. Sub-critical finite amplitude steady motions occur depending on the choice of physical parameters but at higher rotation rates oscillatory convection is found to be the preferred mode of instability. Besides, the stability of steady bifurcating equilibrium solution is discussed using modified perturbation theory. Heat transfer is calculated in terms of Nusselt number. Also, the transient behavior of the Nusselt number is investigated by solving the nonlinear differential equations numerically using the Runge–Kutta–Gill method. It is noted that increase in the value of Taylor number and the couple-stress parameter is to dampen the oscillations of Nusselt number and thereby to decrease the heat transfer.

Keywords Couple-stress fluid · Porous medium · Rotation · Hopf bifurcation · Nonlinear stability

1 Introduction

Thermal convection in fluid-saturated porous media has generated an increasing interest during recent years because of its relevance in a wide range of applications such as water movement in geothermal reservoirs, thermal insulation, solid-matrix compact heat exchangers, energy storage units, ceramic processing and packed bed chemical reactors among others. As a consequence, several studies have been undertaken to investigate the effects of different phenomena connected with such media, and majority of these studies are concerned with Newtonian fluid saturating porous media [1–6].

In the aforementioned applications, the effect of rotation expressed as a Coriolis force plays a vital role. The effect of rotation on the onset of thermal convection in a horizontal fluid layer is well known for ordinary viscous fluids ([7–9], references therein). Its counterpart in a porous layer has also received considerable attention. Friedrich and Rudraiah [10] have studied large amplitude convection in a rotating fluid-saturated porous layer using the Darcy model. Palm and Tyvand [11] have used the same model to study the linear stability

I. S. Shivakumara (✉) · N. Devaraju
UGC-Centre for Advanced studies in Fluid Mechanics, Department of Mathematics,
Bangalore University, Bangalore 560001, India
E-mail: shivakumarais@gmail.com

S. Sureshkumar
Department of Mathematics, Siddaganga Institute of Technology, Tumkur 572103, India

problem of thermal convection in a rotating porous layer, and they have shown that their results are similar to those of nonrotating anisotropic porous medium case. Qin and Kaloni [12] have studied nonlinear stability of the rotating Benard problem in a porous medium by employing the generalized Brinkman model as a suitable prototype for high porosity porous media using energy theory. Vadasz [13] has used linear and weak nonlinear stability theories to study the effect of Coriolis force on gravity-driven convection in a rotating porous layer heated from below by employing the modified Darcy model. The differences as well as similarities between the porous medium and pure fluids convection results are highlighted in this study. An excellent review of research on thermal convection in a rotating porous medium is given by Vadasz [14]. A nonlinear stability analysis for thermal convection in a rotating porous layer has been performed by Straughan [15]. Govender [16] has analyzed the effect of Coriolis force on centrifugally driven convection in a rotating layer of porous medium. Straughan [17] and Malashetty et al. [18] have studied linear and nonlinear thermal convection in a rotating porous layer using a thermal nonequilibrium model. Recently, Shivakumara et al. [19] have investigated the effect of Coriolis force on thermal convection in a layer of Newtonian fluid-saturated porous medium using the Brinkman–Lapwood–Darcy model with fluid viscosity different from Brinkman viscosity.

Although thermal convection in Newtonian fluid-saturated porous media with and without rotational effects has been studied extensively, a limited number of studies are related to thermal convection of non-Newtonian fluids in porous media [20]. With the growing importance of non-Newtonian fluids in modern technology and also of its natural occurrence, the investigations on such fluids are quite desirable. In particular, the theory of polar fluids has received wider attention in recent years because the traditional Newtonian fluids cannot precisely describe the characteristics of the fluid flow encountered in many practical problems such as the extrusion of polymer fluids, solidification of liquid crystals, cooling of metallic plates in a bath, exotic lubricants and colloidal fluids to mention a few. These fluids deform and produce a spin field due to the microrotation of suspended particles forming micropolar fluid developed by Eringen [21]. The micropolar fluids take care of local effects arising from microstructure and as well as the intrinsic motions of microfluidics. The spin field due to microrotation of freely suspended particles set up an antisymetric stress, known as couple-stress, and thus forming couple-stress fluid. Thus couple-stress fluid, according to Eringen [21], is a particular case of micropolar fluid when microrotation balances with the natural vorticity of fluid. The couple-stress fluid has distinct features, such as polar effects and whose microstructure is mechanically significant. For such a special kind of non-Newtonian fluids, the constitutive equations are given by Stokes [22]. Based on this formulation, convective instability in either a couple-stress fluid layer or couple-stress fluid-saturated porous layer heated from below has been investigated in the recent past including the effects of an additional diffusing component (i.e., solute concentration) and external constraints such as magnetic field and /or rotation.

Goel et al. [23] have studied the hydromagnetic stability of an unbounded couple-stress binary fluid mixture under rotation with vertical temperature and solute concentration gradients. A layer of couple-stress fluid saturating a porous medium heated from below in the presence of rotation has been studied by Sharma et al. [24], and condition for the onset of convection is obtained. Sunil et al. [25] have investigated the effect of magnetic field and rotation on a layer of couple-stress fluid heated from below in a porous medium, while Sunil et al. [26] have considered the effect of suspended particles on the stability of a couple-stress fluid layer heated and soluted from below in a porous medium. The linear and nonlinear double diffusive convection with Soret effect in couple-stress liquids have been considered by Malashetty et al. [27]. Gaikwad et al. [28] have studied linear and non-linear double diffusive convection with Soret and Dufour effects in couple-stress liquids. Malashetty et al. [29] have investigated the onset of convection in a couple-stress fluid-saturated porous layer using a thermal nonequilibrium model. Recently, Shivakumara [30] has discussed the effect of various non-uniform basic temperature gradients on the onset of convection in a couple-stress fluid-saturated porous layer.

The interest in the present study is to investigate systematically the effect of Coriolis force on thermal convection in a couple-stress fluid-saturated rotating *rigid* porous layer. Both linear and weakly nonlinear stability analyses have been performed. A truncated model is introduced to construct a system of nonlinear ordinary differential equations with the properties that the linear theory and the finite amplitude solutions obtained up to second order in the amplitude expansion will be identical to those obtained in the case of full problem. From the study of linear stability analysis, condition for the occurrence of different types of bifurcations is obtained. The presence of rotation gives rise to oscillatory convection and more interestingly it is recognized that the couple-stress parameter plays a dual role on the stability of the system in the presence of rotation; a result not noticed in its absence. By performing weakly nonlinear stability analysis, it is established that sub-critical motions are possible for a suitable choice of physical parameters. Besides, the nonlinear system of autonomous ordinary differential equations are solved numerically using the Runge–Kutta–Gill method with appropriate initial conditions to know the transient behavior of heat transport which is calculated in terms of Nusselt number. The existing results for the Newtonian fluid are obtained as particular cases in the present study.

2 Mathematical formulation

We consider an infinite horizontal layer of couple-stress fluid-saturated porous medium confined between horizontal planes at $z = 0$, *d and the solid phase of the porous medium is considered to be rigid*. The temperatures of the lower and upper surfaces bounding the porous medium are taken to be uniform and equal to $T_0 + \Delta T$ and T_0, respectively, with $\Delta T > 0$. The entire system is rotating with constant angular velocity $\vec{\Omega} = \Omega\hat{k}$, where $\hat{k}$ is a unit vector in the vertical direction, *and the rotation does not disrupt the isotropy of the rigid porous medium*. It is assumed that the fluid and solid phases of the porous medium are in local thermal equilibrium. A Cartesian coordinate system (*x, y, z*) is used, with the *z*-axis vertically upward in the gravitational field. The Boussinesq approximation is assumed to be valid, and the equation of continuity and state is, respectively, given by:

$$\nabla \cdot \vec{q} = 0 \tag{1}$$

$$\rho = \rho_0\{1 - \alpha_t(T - T_0)\} \tag{2}$$

where, $\vec{q} = (u, v, w)$ is the seepage velocity vector, T the temperature, ρ the fluid density and α_t the thermal expansion coefficient. The energy equation is given by

$$A_h \frac{\partial T}{\partial t} + (\vec{q} \cdot \nabla)T = \kappa \nabla^2 \vec{q} \tag{3}$$

where $A_h = (\rho_0 c)_m/(\rho_0 c)_f = [(1-\varepsilon)(\rho_0 c)_s + \varepsilon(\rho_0 c)_f]/(\rho_0 c)_f$ the ratio of heat capacities, κ the effective thermal diffusivity, c the specific heat and ε the porosity. The subscripts m, s and f refer to the porous medium, solid and fluid, respectively.

Following Stokes [22], the equation of motion of an incompressible couple-stress fluid in the absence of body couple and a porous medium is:

$$\rho_0 \left[\frac{\partial \vec{q}_f}{\partial t} + \left(\vec{q}_f \cdot \nabla\right) \vec{q}_f \right] = -\nabla p + \rho \vec{g} + \mu \nabla^2 \vec{q}_f - \mu_c \nabla^4 \vec{q}_f \tag{4}$$

where $\vec{q}_f$ is the velocity of couple-stress fluid in the absence of porous medium, p the fluid pressure, μ the dynamic viscosity, μ_c the material constant responsible for the couple-stress property known as the couple-stress viscosity and $\vec{g}$ the acceleration due to gravity. In the case of polar fluids the action of one part of the body on its neighborhood cannot be represented by a force alone but rather by a force and couple. The last term on the right-hand side of Eq. (4) represents the effect of couple-stresses in an incompressible fluid. When $\mu_c = 0$, Eq. (4) reduces to the Navier–Stokes equation. The equation of motion of couple-stress fluid through a porous medium can be viewed as follows. It is a known fact that the Darcy equation can be derived from the Navier–Stokes equation by statistical averages and simplifications of the complicated microscopic flow picture [31,32]. Following the same procedure, the equation of motion for a couple-stress fluid through a porous medium can be obtained from Eq. (4), and with the inclusion of rotational effects the equation reads as

$$\frac{1}{\varepsilon}\frac{\partial \vec{q}}{\partial t} = -\frac{1}{\rho_0}\nabla P + \{1 - \alpha_t(T - T_0)\}\vec{g} - \frac{2}{\varepsilon}\vec{\Omega} \times \vec{q} - \frac{1}{k\rho_0}\left(\mu - \mu_c \nabla^2\right)\vec{q} \tag{5}$$

where $\vec{q} = \varepsilon \vec{q}_f$, P is the effective pressure and k is the permeability of the porous medium. Equation (5) is indeed the averaged equation applicable for couple-stress fluid flow through rotating porous media. It is observed that the presence of rotation introduces an additional body force known as Coriolis force which has a profound effect on the flow of couple-stress fluid through porous media. The time derivative term is taken into consideration in Eq. (5) in order to analyze the occurrence of oscillatory convection due to the presence of rotation. When $\mu_c = 0$, Eq. (5) reduces to the case of Newtonian fluid saturating a porous medium and note that the presence of couple-stress is to alter the viscosity of the fluid. Thus, the governing equations which are needed to solve the problem under discussion are Eqs. (1), (3) and (5), which are, respectively, the continuity equation, the energy equation and the momentum equation.

The basic state is quiescent, and the basic temperature distribution satisfying the boundary conditions $T_b = T_0 + \Delta T$ at $z = 0$ and $T_b = T_0$ at $z = d$ is given by $T_b - T_0 = \Delta T(1 - z/d)$, where the subscript b denotes the basic state. We restrict our attention to two-dimensional convection in the perturbed state, and all variations with respect to y are assumed to vanish. For the present configuration, it is convenient to eliminate the pressure P by cross-differentiating the first and the third equations of motion given by Eq. (5). Then defining the y-component of vorticity, $\zeta = \partial u/\partial z - \partial w/\partial x$, we have

$$\frac{1}{\varepsilon}\frac{\partial \zeta}{\partial t} - \frac{2\Omega}{\varepsilon}\frac{\partial v}{\partial z} = -\alpha_t g \frac{\partial \theta}{\partial x} - \frac{1}{\rho_0 k}(\mu - \mu_c \nabla^2)\zeta \tag{6}$$

where, $\theta\ (x, z, t)$ is the deviation of the temperature from the linear profile.

The second equation of motion has the form

$$\frac{1}{\varepsilon}\frac{\partial v}{\partial t} + \frac{2\Omega}{\varepsilon} u = -\frac{1}{\rho_0 k}(\mu - \mu_c \nabla^2) v. \tag{7}$$

Introducing the stream function ψ through the definition $u = \partial\psi/\partial z$, $w = -\partial\psi/\partial x$ and non-dimensionalizing the variables by scaling t by $d^2\varepsilon/\kappa$, $\vec{q}$ by κ/d, x and z by d and θ by ΔT, we obtain the following dimensionless equations

$$\left[\frac{1}{Pr_D}\frac{\partial}{\partial t} + \left(1 - \Lambda_c \nabla^2\right)\right]\nabla^2\psi = Ta_D^{1/2}\frac{\partial v}{\partial z} - R_D \frac{\partial \theta}{\partial x} \tag{8}$$

$$\left(\frac{1}{Pr_D}\frac{\partial}{\partial t} + \left(1 - \Lambda_c \nabla^2\right)\right) v = -Ta_D^{1/2}\frac{\partial \psi}{\partial z} + \frac{1}{Pr_D} J(\psi, v) \tag{9}$$

$$\left(M\frac{\partial}{\partial t} - \nabla^2\right)\theta = -\frac{\partial \psi}{\partial z} + J(\psi, \theta) \tag{10}$$

where, $J\ (f, g) = \frac{\partial f}{\partial x}\frac{\partial g}{\partial z} - \frac{\partial f}{\partial z}\frac{\partial g}{\partial x}$ is the Jacobian, $R_D = \alpha_t g \Delta T k d/\nu\kappa$ is the Darcy–Rayleigh number, $Ta_D = 4\Omega^2 k^2/\nu^2\varepsilon^2$ is the Darcy-Taylor number, $Pr_D = \nu\varepsilon^2 d^2/k\kappa$ is the modified Darcy–Prandtl number, $M = A_h/\varepsilon$ is the non-dimensional group, $\Lambda_c = \mu_c/\mu d^2$ is the couple-stress parameter and $\nu = \mu/\rho_0$ is the kinematic viscosity. It may be noted that the system behaves like a double diffusive one with angular velocity as a second component. The effects of couple-stress are significant for large values of $\Lambda_c(=l/d)$, where $l = \sqrt{\mu_c/\mu}$ is the material constant. If l is a function of the molecular dimensions of the liquid, it will vary greatly for different liquids. For example, the length of a polymer chain may be a million times the diameter of water molecule [22]. Therefore, there are all the reasons to expect that couple-stresses appear in noticeable magnitudes in liquids with large molecules.

We have to solve Eqs. (8), (9) and (10) subject to the boundary conditions. The boundaries are assumed to be impermeable with vanishing couple-stress and perfect conductor of heat. Therefore, the boundary conditions are as follows:

$$\psi = \frac{\partial^2 \psi}{\partial z^2} = \frac{\partial v}{\partial z} = 0 \quad \text{at } z = 0, 1 \tag{11a}$$

$$\theta = 0 \quad \text{at } z = 0, 1. \tag{11b}$$

Although it is possible to solve Eqs. (8), (9) and (10) subject to the boundary conditions numerically, here we construct a set of coupled nonlinear ordinary differential equations with solutions that mimic the essential features of solution to the full system. For this, we expand the dependent variables as truncated double Fourier series in space and then adopt the minimal representation such that-

(i) the linear theory results are identical with those for the full problem,
(ii) the seepage velocity remains finite for all finite values of R_D, and
(iii) some effects of zonal velocity are included.

These are achieved with a fifth-order system of nonlinear ordinary differential equations which possesses both periodic and steady solutions and allows sub-critical instability. This simplified model has the great advantage that steady finite amplitude solutions can be obtained at once and their stability can be investigated analytically. Moreover, the representation is just that which reproduces results obtained by modified perturbation theory to second order in amplitude, for the full problem and qualitatively accurate for larger amplitudes. Following the procedure introduced by Veronis [33] and Moroz [34], we construct a low-order model that allows us to study the linear and weakly nonlinear aspects of the problem. Accordingly, the stream function, the temperature and the zonal velocity are expanded as Fourier series in x and z as follows:

$$\psi = \frac{2\sqrt{2}}{\alpha}\delta A(t^*)\sin(\alpha x)\sin(\pi z) \tag{12a}$$

$$\theta = \frac{2\sqrt{2}}{\delta}B(t^*)\cos(\alpha x)\sin(\pi z) - \frac{C(\tau)}{\pi}\sin(2\pi z) \tag{12b}$$

$$v = \frac{2\sqrt{2}}{\alpha\delta}D(t^*)\sin(\alpha x)\cos(\pi z) - \frac{E(\tau)}{\pi}\sin(2\alpha x) \tag{12c}$$

where α is the wave number, $\delta^2 = \pi^2 + \alpha^2$ is the total wave number, $t^* = \delta^2 t$ is the normalized time and $A(t^*) - E(t^*)$ are the amplitudes which are to be determined in the dynamics of the system. These fields are consistent with the respective boundary conditions. Substituting the above expressions into Eqs. (8), (9) and (10) and consistently neglecting all terms generated that involve higher harmonics, we obtain a system of autonomous nonlinear ordinary differential equations in the following form:

$$\frac{dA}{dt^*} = -Pr_D\left[\eta A + \frac{R_D\alpha^2}{\delta^6}B - \frac{\pi Ta_D^{1/2}}{\delta^6}D\right] \tag{13a}$$

$$\frac{dB}{dt^*} = \frac{1}{M}\left[A(C-1) - B\right] \tag{13b}$$

$$\frac{dC}{dt^*} = -\frac{\beta}{M}(AB + C) \tag{13c}$$

$$\frac{dD}{dt^*} = -\left(Pr_D\eta D + Pr_D\pi Ta_D^{1/2}A + \alpha AE\right) \tag{13d}$$

$$\frac{dE}{dt^*} = -\frac{Pr_D}{\delta^2}\varpi E + \frac{\beta AD}{\alpha} \tag{13e}$$

where $\eta = 1/\delta^2 + \Lambda_c$, $\beta = 4\pi^2/\delta^2$ and $\varpi = 1 + 4\Lambda_c\alpha^2$. We note that η is a representative of the viscosity of the fluid, and it is evident that the suspended particles add to the viscosity. The truncation leading to the above equations is consistent, in that no other lower-order harmonics are generated by the substitutions (12a–c). Equations (13a–e) are the basic set that will be studied in this paper. These equations possess two significant properties. First, the divergence of the flow in phase space

$$\frac{\partial\dot{A}}{\partial A} + \frac{\partial\dot{B}}{\partial B} + \frac{\partial\dot{C}}{\partial C} + \frac{\partial\dot{D}}{\partial D} + \frac{\partial\dot{E}}{\partial E} = -\left[Pr_D\left(2\eta + \frac{\varpi}{\delta^2}\right) + \frac{(1+\beta)}{M}\right] \tag{14}$$

where dot above a quantity denotes derivative with respect to t^*, is always negative and so the solutions are attracted to a set of measure zero in the phase space. This may be a fixed point, a limit cycle or a strange attractor. Second, the equations have an important symmetry, for they are unchanged if the signs of A, B and D are reversed while C and E are left unchanged. More generally, the Fourier expansion in x and z leads to an infinite set of coupled nonlinear ordinary differential equations. The truncation (12a–c) does in fact include just those Fourier components that appear when A is small.

3 Linear stability analysis

Equation (13a–e) admit the trivial solution $A = B = C = D = E = 0$ that corresponds to pure conduction of heat with no fluid motion present. The linear stability of this static solution may be obtained from the system Eq. (13a–e) by neglecting all nonlinear terms and seeking the solutions of the form $\exp(\sigma t^*)$, where $\sigma = \omega_r + i\omega$ is a complex number, whose real part represents the growth rate and imaginary part allows for an oscillatory behavior. No instability arises from the decoupled equations for C and E, and the remaining three equations yield the cubic dispersion relation

$$\sigma^3 + \delta_1\sigma^2 + \delta_2\sigma + \delta_3 = 0 \tag{15}$$

Table 1 Variation of $\alpha^2_{\min}$ for different values of Λ_c and Ta_D

Ta_D	0	50	100	200
Λ_c	$\alpha^2_{\min}$	$\alpha^2_{\min}$	$\alpha^2_{\min}$	$\alpha^2_{\min}$
0	3.142	8.395	9.959	11.829
0.5	2.289	2.788	3.083	3.469
1.0	2.257	2.442	2.586	2.808
1.5	2.246	2.339	2.420	2.558
2.0	2.239	2.295	2.346	2.438

where,

$$\delta_1 = \delta^2\left(2Pr_D\eta + \frac{1}{M}\right) \tag{16a}$$

$$\delta_2 = \frac{Pr_D\alpha^2}{M\delta^2}\left(\frac{\delta^6 Pr_D M\eta^2}{\alpha^2} + \frac{2\delta^6\eta}{\alpha^2} + \frac{\pi^2 Pr_D Ta_D M}{\alpha^2} - R_D\right) \tag{16b}$$

$$\delta_3 = \frac{Pr_D^2\alpha^2\eta}{M}\left(\frac{\delta^6\eta}{\alpha^2} + \frac{\pi^2 Ta_D}{\alpha^2\eta} - R_D\right). \tag{16c}$$

The roots of Eq. (15) give different bifurcations and these are discussed in the following subsections.

3.1 Codimension-one stationary bifurcation

This type of bifurcation corresponds to a simple zero eigenvalue (i.e., $\sigma = 0$), which can be obtained when $\delta_3 = 0$ and $\delta_2 > 0$. The condition $\delta_3 = 0$ gives the simple bifurcation. The simple bifurcation occurs at $R_D = R_D^s$, where

$$R_D^s = \frac{\delta^6\eta}{\alpha^2} + \frac{\pi^2 Ta_D}{\alpha^2\eta}. \tag{17}$$

To find the minimum value of R_D^s, it is differentiated with respect to α^2 and equated to zero. A polynomial in $\alpha^2_{\min}$, whose coefficients are functions of the parameters influencing the instability, is obtained and is given by

$$2\left(\alpha^2_{\min}\right)^5 + 5\left(\eta' + \frac{2\pi^2}{5}\right)\left(\alpha^2_{\min}\right)^4 + 4\eta'\left(\eta' + \pi^2\right)\left(\alpha^2_{\min}\right)^3 + \left\{\eta'^2 + 2\pi^2\eta' - \pi^4 - \frac{Ta_D\pi^2}{\Lambda_c}\right\}\left(\alpha^2_{\min}\right)^2 - \pi^4\left(\eta'^2 + \frac{Ta_D}{\Lambda_c^2}\right)\left(2\alpha^2_{\min} + \eta'\right) = 0 \tag{18}$$

where, $\eta' = \pi^2 + 1/\Lambda_c$. The values of $\alpha^2_{\min}$ computed numerically for different values of Λ_c and Ta_D are tabulated in Table 1. From this table it is seen that increase in the value of couple-stress parameter is to decrease marginally the critical wave number, and hence its effect is to enlarge the size of convection cells. However, increase in the value of Ta_D is to increase the wave number, but significantly when the couple-stresses are absent (i.e., $\Lambda_c = 0$). Also, from Eq. (17) it is seen that the presence of Coriolis effect is to increase the value of R_D^s, and hence it has a stabilizing effect on the system.

When $Ta_D = 0$, Eq. (17) reduces to

$$R_D^s = \frac{\delta^6}{\alpha^2}\left(\frac{1}{\delta^2} + \Lambda_c\right). \tag{19}$$

We note that R_D^s given by Eq. (19) attains its minimum value at

$$\alpha_{\min} = \sqrt{\left\{\frac{-\left(\pi^2\Lambda_c + 1\right) + \sqrt{\left(\pi^2\Lambda_c + 1\right)\left(9\pi^2\Lambda_c + 1\right)}}{4\Lambda_c}\right\}} \tag{20}$$

By rescaling the quantities in the form $R^s_{Dres} = R^s_D/\pi^2$, $\Lambda = \Lambda_c\pi^2$, and $a = \alpha^2/\pi^2$, Eq. (17) can be written as

$$R^s_{Dres} = \frac{(1+a)Ta_{Dres}}{a[1+\Lambda(1+a)]} + \frac{(1+a)^2}{a} + \frac{(1+a)^3\Lambda}{a}. \tag{21}$$

When Λ_c=0 (i.e., Newtonian fluid case), Eq. (21) reduces to

$$R^s_{Dres} = \frac{(1+a)^2}{a} + \frac{(1+a)}{a}Ta_{Dres} \tag{22}$$

and coincides with the results of Vadasz [13].

3.2 Codimension-one Hopf bifurcation

This type of bifurcation occurs when $\delta_3 = \delta_1\delta_2$ and $\delta_2 > 0$. Then, a pair of complex conjugate eigenvalues $\sigma = \pm i\omega$ is a possible solution of Eq. (15). This corresponds to an oscillatory instability. The condition $\delta_3 = \delta_1\delta_2$ gives an expression for the Rayleigh number $R_D = R^H_D$ at which Hopf bifurcation occurs, where

$$R^H_D = \frac{2\eta\,(1+Pr_D\eta M)}{\alpha^2}\left[\delta^6 + \lambda^2\pi^2 Ta_D\left(\frac{Pr_D}{1+Pr_D\eta M}\right)^2\right]. \tag{23}$$

The second condition gives the oscillation frequency ω^2 as a function of physical parameters as

$$\omega^2 = \frac{(1-Pr_D\eta M)\,Pr^2_D\pi^2 Ta_D}{\delta^2\,(1+Pr_D\eta M)} - \delta^4 Pr^2_D\eta^2. \tag{24}$$

For the occurrence of Hopf bifurcation ω^2 must be positive. From the above equation it is thus evident that Hopf bifurcation is not possible if the Coriolis effect is not present (i.e., $Ta_D = 0$). In other words, the Coriolis force due to rotation is the cause to set up oscillatory convection in a couple-stress fluid - saturated *rigid* porous medium as observed in the Newtonian fluids. Since $\omega^2 > 0$, from Eq. (24) it is clear that the necessary conditions for the occurrence of oscillatory instability are

$$Pr_D < \frac{1}{\eta M}, \quad Ta_D > \frac{\delta^6\eta^2\,(1+Pr_D\eta M)}{\pi^2\,(1+Pr_D\eta M)}. \tag{25}$$

We note that the oscillatory instability can appear only when the Taylor number exceeds a threshold value which in turn depends on the couple-stress parameter, modified Darcy–Prandtl number and parameter M. Further, it is interesting to note that Eq. (24) is equivalent to

$$\omega^2 = \frac{Pr^2_D\eta\alpha^2}{\delta^2\,(1+2Pr\eta M)}\left(R^s_D - R^H_D\right). \tag{26}$$

From Eq. (26) it is evident that if Hopf bifurcation is possible, it always occurs at a lower value of the Rayleigh number at which the simple bifurcation occurs. By rescaling the quantities, Eqs. (23) and (24) can be expressed, respectively, in the form

$$R^H_{Dres} = \frac{2[1+\Lambda(1+a)]}{a}\left[(1+a)\,\{(1+a)+\gamma M[1+\Lambda(1+a)]\} + \frac{\gamma^2 M^2 Ta_{Dres}}{\{(1+a)[1+\gamma\Lambda M]+\gamma M\}}\right] \tag{27}$$

and

$$\omega^2_{res} = \frac{[1+a-\gamma M\{1+\Lambda(1+a)\}]Ta_{Dres}}{(1+a)\{(1+a)[1+\gamma M\Lambda]+\gamma M\}} - [1+\Lambda(1+a)]^2 \tag{28}$$

where, $\gamma = Pr_D/\pi^2$, $\omega^2_{res} = \omega^2/Pr^2_D$ and other quantities have their pre-defined meaning.

When $\Lambda_c = 0$ (i.e., Newtonian fluid case), Eqs. (27) and (28), respectively, reduce to

$$R_D^H = \frac{2}{a}\left[(1+a)(1+a+\gamma M) + \frac{\gamma^2 M^2 Ta_{Dres}}{(1+a+\gamma M)}\right] \tag{29}$$

and

$$\omega_{res}^2 = \frac{(1+a-\gamma M)\, Ta_{Dres}}{(1+a)(1+a+\gamma M)} - 1 \tag{30}$$

which coincide with those of Vadasz [13].

3.3 Codimension-two (CT) stationary bifurcation

This type of bifurcation occurs when $\delta_2 = 0 = \delta_3$. Then, Eq. (15) reduces to $\sigma^2(\sigma+\delta_1) = 0$, and find $\sigma = 0$, 0 (a double zero) and $\sigma = -\delta_1$ (stable) are the solutions of this equation. The conditions $\delta_2 = 0 = \delta_3$ give the following relations

$$\frac{\eta\delta^6}{a^2}(Pr_D M\eta + 1) + \frac{\pi^2 Ta_D}{a^2\eta}(Pr_D\eta M - 1) = 0 \tag{31}$$

and

$$R_D^H = R_D^s = R_{CT} = \frac{\delta^6\eta}{\alpha^2} + \frac{\pi^2 Ta_D}{\alpha^2\eta}. \tag{32}$$

3.4 Codimension-two Hopf bifurcation

This type of bifurcation can be obtained with $\delta_3 = 0$, $\delta_1 = 0$ and $\delta_2 > 0$. Then the solutions are $\sigma = 0$ and $\sigma = \pm i\omega$, and in this case there is competition between stationary and oscillatory instability. Nevertheless, from Eq. (16a) it is evident that δ_1 is always greater than zero and hence this type of bifurcation is not possible in the present problem.

4 Weakly nonlinear stability analysis

The system (13a–e) is nonlinear, and analytical solutions are not possible. However, we can obtain the solution for the steady state. Such a study is useful because it predicts whether a finite amplitude steady solution for the system is possible for sub-critical values of the Rayleigh number or otherwise.

Setting the left-hand sides of Eq. (13a–e) equal to zero, we have

$$0 = \eta A + \frac{R_D\alpha^2}{\delta^6}B - \frac{\pi Ta_D^{1/2}}{\delta^2}D \tag{33a}$$

$$0 = A(C-1) - B \tag{33b}$$

$$0 = AB + C \tag{33c}$$

$$0 = \eta D + Pr_D\pi Ta_D^{1/2}A + \alpha AE \tag{33d}$$

$$0 = -\frac{Pr_D}{\delta^2}\varpi E + \frac{\beta AD}{\alpha}. \tag{33e}$$

The above equations admit a nontrivial solution defined for all amplitudes A of the motion. This solution is given by

$$B = -\frac{A}{A^2 + 1} \tag{34a}$$

$$C = \frac{A^2}{A^2 + 1} \tag{34b}$$

$$D = -\frac{Pr_D^2 \pi Ta_D^{1/2} \varpi A}{Pr_D^2 \eta \varpi + 4\pi^2 A^2} \tag{34c}$$

$$E = -\frac{4\pi^3 Pr_D Ta_D^{1/2} A^2}{\alpha \left(Pr_D^2 \eta \varpi + 4\pi^2 A^2\right)}. \tag{34d}$$

Substituting for B and D thus obtained in Eq. (33a) yields the equation

$$A\left[4\pi^2 \eta \left(A^2\right)^2 + L_1 \left(A^2\right) + L_2\right] = 0 \tag{35a}$$

where

$$L_1 = Pr_D^2 \varpi \left(\eta^2 + \frac{\pi^2 Ta_D}{\delta^6}\right) + 4\pi^2 \left(\eta - \frac{R_D \alpha^2}{\delta^6}\right) \tag{35b}$$

$$L_2 = Pr_D^2 \varpi \alpha^2 \left(R_D^s - R_D\right). \tag{35c}$$

The solution $A = 0$ corresponds to pure conduction, and the remaining solutions are given by

$$A^2 = \frac{\left[-L_1 \pm \left(L_1^2 - 16\pi^2 \eta L_2\right)^{1/2}\right]}{8\pi^2 \eta}. \tag{36}$$

We note that if L_1 is negative, then L_2 will also be negative. Hence, the solution only with positive sign in front of the radical is admissible, otherwise A^2 becomes negative. Consider the case when finite amplitude solutions exist for $R_D < R_D^s$. The minimum value of R_D for which finite amplitude solutions exist is that value of R_D which makes the radical vanishes provided L_1 is non-negative. The radical vanishes provided that

$$R_D = R_D^f = \frac{\delta^6}{4\pi^2 \alpha^2} \left[\frac{Pr_D \pi Ta_D^{1/2} \varpi^{1/2}}{\delta^3} + \left\{\eta \left(4\pi^2 - Pr_D^2 \eta \varpi\right)\right\}^{1/2}\right]^2 \tag{37}$$

where R_D^f is called the finite amplitude Darcy–Rayleigh number, which characterizes the onset of finite amplitude steady motions. Equation (37) gives meaningful result only when

$$Pr_D < Pr_{D1} = \frac{2\pi}{\sqrt{\eta \varpi}}. \tag{38}$$

Thus, for fluids with Prandtl number greater than Pr_{D1} sub-critical motions are not possible.

After rescaling the quantities as before, Eq. (38) can be expressed in the form

$$R_{Dres}^f = \frac{1}{4a} \left[\gamma \chi Ta_{Dres}^{1/2} + \{(1+a)[1 + \Lambda(1+a)][4(1+a) - \gamma^2 \chi [1 + \Lambda(1+a)]\}^{1/2}\right]^2 \tag{39}$$

where $R_{Dres}^f = R_D^f / \pi^2$, $\chi = \sqrt{(1 + 4\Lambda a)}$ and other quantities have their pre-defined meaning. When $\Lambda_c = 0$ (i.e., Newtonian fluid case), Eq. (39) reduces to

$$R_{Dres}^f = \frac{1}{4a} \left[\gamma Ta_{Dres}^{1/2} + \left\{(1+a)\left(4 + 4a - \gamma^2\right)\right\}^{1/2}\right]^2. \tag{40}$$

5 Modified perturbation theory

In the neighborhood of R^s_D there is a triplet of steady solutions, one of which is the static solution. The other two are finite amplitude solutions which, due to the symmetry of Eq. (13a–e), differ only in the sign of A, B and D. We may investigate the stability of the two branches of non-trivial steady solutions in the neighborhood of R^s_D in terms of the seepage velocity amplitude A by setting

$$R = R^s_D + R^s_{D2}\left(A^2\right) + \cdots \tag{41}$$

for $A^2 << 1$. Substituting Eq. (41) into Eq. (35a), one finds, for zeroth order in A^2, the results of linear stability analysis as obtained in Sect. 3.1.

To the first order in A^2, we then find that

$$R^s_{D2} = \frac{\eta\delta^6}{\alpha^2} + \frac{\pi^2 Ta_D\left(Pr_D^2\eta\varpi - 4\pi^2\right)}{Pr_D^2\eta^2\alpha^2\varpi}. \tag{42}$$

We note that R^s_{D2} may be either positive or negative. The finite amplitude solution is said to be stable (i.e., supercritical) if $R^s_{D2} > 0$ and unstable (i.e., sub-critical) if $R^s_{D2} < 0$, when $\omega^2 < 0$.

From Eq. (42) it is clear that the finite amplitude solution is stable provided

$$Pr_D > Pr_{D1} = \frac{2\pi}{\sqrt{\eta\varpi}} \tag{43}$$

a result which is consistent with the one obtained earlier (see Eq. 38). In the absence of rotation (i.e., $Ta_D = 0$), we find that $R^s_{D2} = R^s_D$, and hence sub-critical instability is not possible.

After rescaling the quantities, Eq. (42) can be expressed in the form

$$R^s_{D2res} = \frac{(1+a)^2}{a}\{1+\Lambda(1+a)\} + Ta_{Dres}\frac{(1+a)\{\gamma^2[1+\Lambda(1+a)](1+4\Lambda a) - 4(1+a)\}}{a\gamma^2[1+\Lambda(1+a)]^2(1+4\Lambda a)} \tag{44}$$

where $R^s_{D2res} = R^s_{D2}/\pi^2$ and the other quantities have their pre-defined meaning.

When $\Lambda_c = 0$ (i.e., Newtonian fluid case), Eq. (44) reduces to

$$R^s_{D2res} = \frac{(1+a)^2}{a} + Ta_{Dres}\frac{(1+a)\left(\gamma^2 - 4a - 4\right)}{a\gamma^2}. \tag{45}$$

6 Heat transport

The vigor of convection can be measured in terms of either the heat flux or the kinetic energy. It is convenient to introduce a normalized heat flux, given by the Nusselt number

$$Nu = -\left\langle \frac{\partial T}{\partial z} \right\rangle_{z=0} \tag{46}$$

where, the angle brackets $\langle\cdots\rangle$ correspond to a horizontal average. Substituting for $T = -z + \theta$ in Eq. (46), we obtain

$$Nu = 1 + 2C. \tag{47}$$

Substituting for the amplitude C in terms of A, we obtain

$$Nu = 1 + \frac{2A^2}{A^2+1}. \tag{48}$$

For small amplitude convection, we have

$$A^2 = \frac{R_D - R^s_D}{R^s_{D2}}. \tag{49}$$

When $A = 0 (i.e.,\ R_D = R^s_D)\ Nu = 1$ and hence the heat transport is only by conduction.

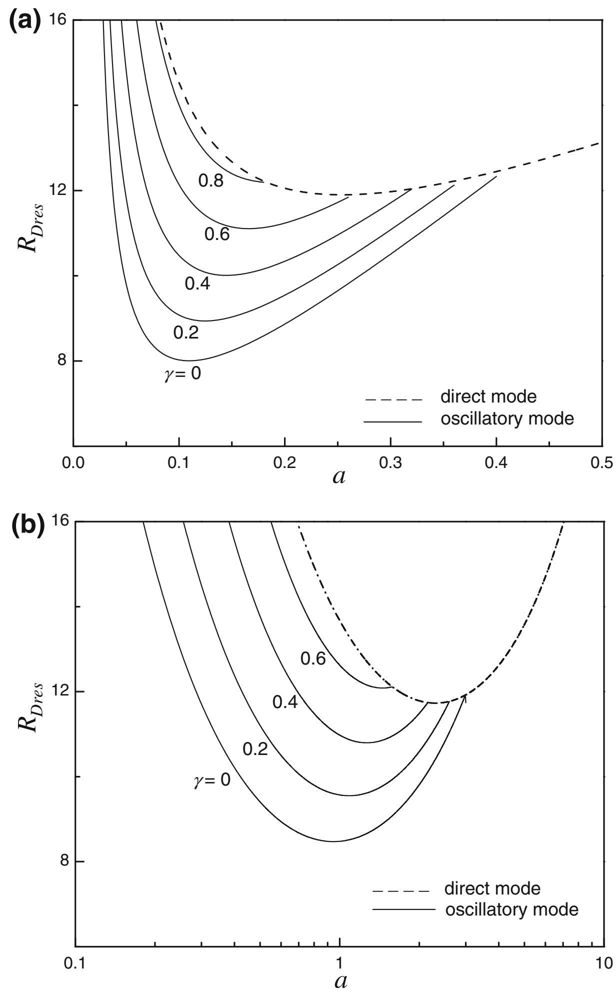

Fig. 1 Neutral stability *curves* for different values of γ with $Ta_{Dres} = 5$ for **a** $\Lambda = 0$ and **b** $\Lambda = 0.03$

7 Results and discussion

The linear and weakly nonlinear thermal convection in a horizontal couple-stress fluid-saturated rotating *rigid* porous layer are investigated. The primary effect of rotation is to introduce oscillatory convection in a couple-stress fluid-saturated porous layer. In the case of linear stability theory, the condition for the occurrence of different types of bifurcation is obtained. By carrying out the nonlinear stability analysis, the possibility of occurring sub-critical motion is analyzed. Besides, heat transfer is calculated in terms of Nusselt number. The results obtained are presented graphically in Figs. 1, 2, 3, 4, 5, 6, 7 and 8.

Figures 1 and 2 show the marginal stability curves for steady and oscillatory modes in the (R_{Dres}, a)-plane for $Ta_{Dres} = 5$ and 10, respectively, for different values of modified Prandtl number γ with $M = 1.25$ when $\Lambda = 0$ (i.e., Newtonian fluid) and 0.03. The results presented in Figs. 1a and 2a are for $\Lambda = 0$, while for $\Lambda = 0.03$ the results are shown in Figs. 1b and 2b. From these figures, we note that the neutral curves are connected in a topological sense and the oscillatory mode is found to be the preferred mode of instability only up to a certain value of γ which in turn depends on the strength of rotation (Ta_{Dres}) as well as couple-stresses (Λ). Further inspection of the figures shows that the range of γ up to which the oscillatory mode is preferred decreases in the presence of couple-stresses when compared to its absence (see Fig. 1a, b), while the range of γ increases with an increase in the value of Ta_{Dres} irrespective of couple-stress effects. Moreover, increase in the value of γ is to increase the critical oscillatory Darcy–Rayleigh number and thus it has a stabilizing effect on the system, and the case of $\gamma \to 0$ provides a lower bound for the oscillatory neutral curves.

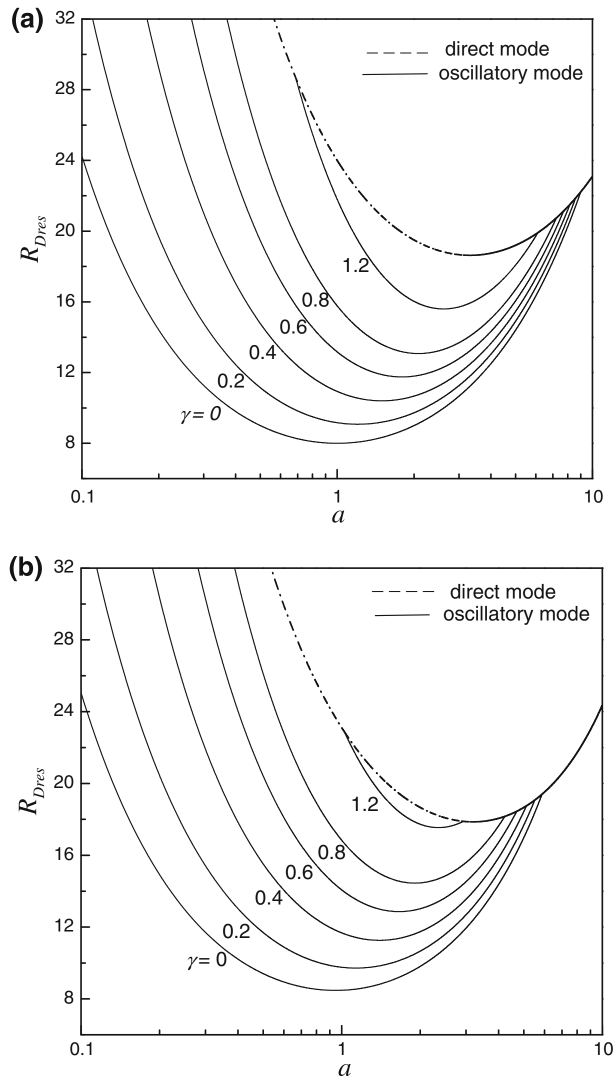

Fig. 2 Neutral stability *curves* for different values of γ with $Ta_{Dres} = 10$ for **a** $\Lambda = 0$ and **b** $\Lambda = 0.03$

Besides, the critical wave number increases (i.e., the size of convection cell decreases) with increasing γ, and also the critical wave number for the direct mode is higher than that of oscillatory mode.

From Eqs. (21), (27) and (37), we, respectively, note that

$$\frac{\partial R_{Dres}^{s}}{\partial Ta_{Dres}} = \frac{(1+a)}{a[1+\Lambda(1+a)]} > 0 \tag{50}$$

$$\frac{\partial R_{Dres}^{H}}{\partial Ta_{Dres}} = \frac{2[1+\Lambda(1+a)]\gamma^2 M^2}{a\{(1+a)[1+\gamma\Lambda M]+\gamma M\}} > 0 \tag{51}$$

$$\frac{\partial R_{D}^{f}}{\partial Ta_{Dres}} = \frac{\gamma\chi\left[\gamma\chi Ta_{Dres}^{1/2} + \{(1+a)[1+\Lambda(1+a)][4(1+a)-\gamma^2\chi[1+\Lambda(1+a)]\}^{1/2}\right]}{4aTa_{Dres}^{1/2}} > 0. \tag{52}$$

Thus, R_{Dres}^{s}, R_{Dres}^{H} and R_{Dres}^{f} are increasing functions of Ta_{Dres}, and hence the effect of rotation is to reinforce stabilizing effect on the system. However, we note that

$$\frac{\partial R_{Dres}^{s}}{\partial \Lambda} = \frac{(1+a)^3}{a} - \frac{(1+a)^2 Ta_{Dres}}{a[1+\Lambda(1+a)]^2}. \tag{53}$$

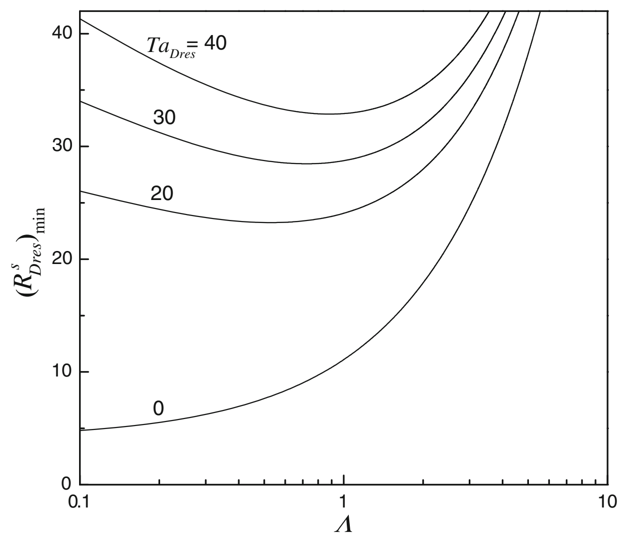

Fig. 3 Variation of $\left(R^s_{Dres}\right)_{\min}$ as a function of Λ for different values of Ta_{Dres}

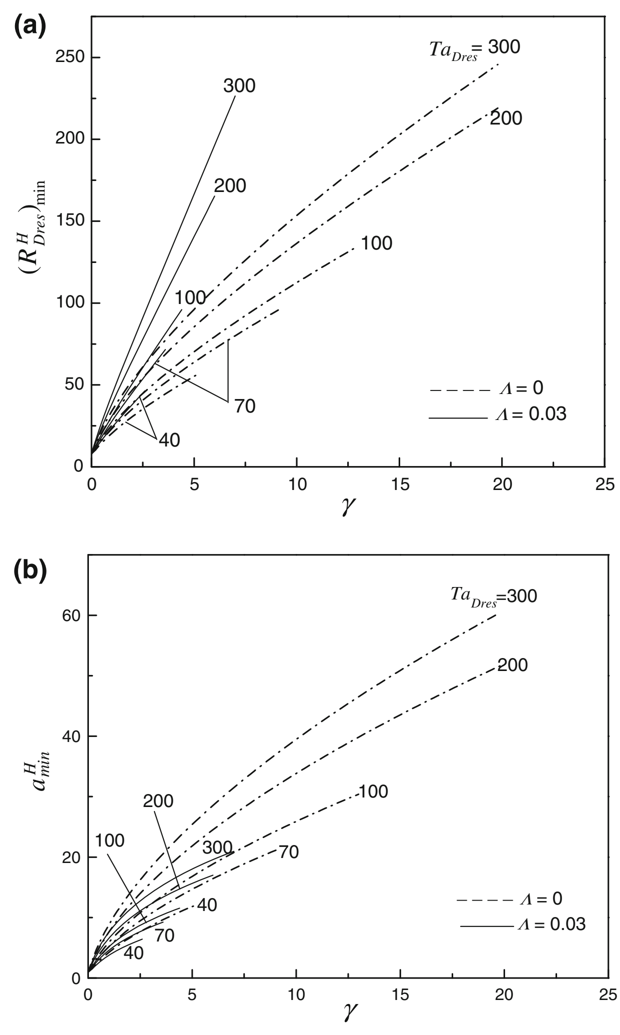

Fig. 4 Variation of **a** $\left(R^H_{Dres}\right)_{\min}$ and **b** $a^H_{\min}$ associated with oscillatory convection as a function of γ for different values of Ta_{Dres}

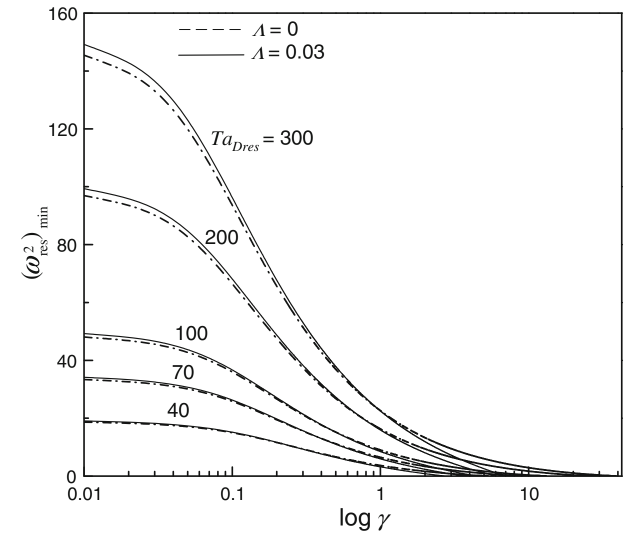

Fig. 5 Variation of $\left(\omega^2_{\text{res}}\right)_{\min}$ associated with oscillatory convection as a function of logγ for different values of Ta_{Dres}

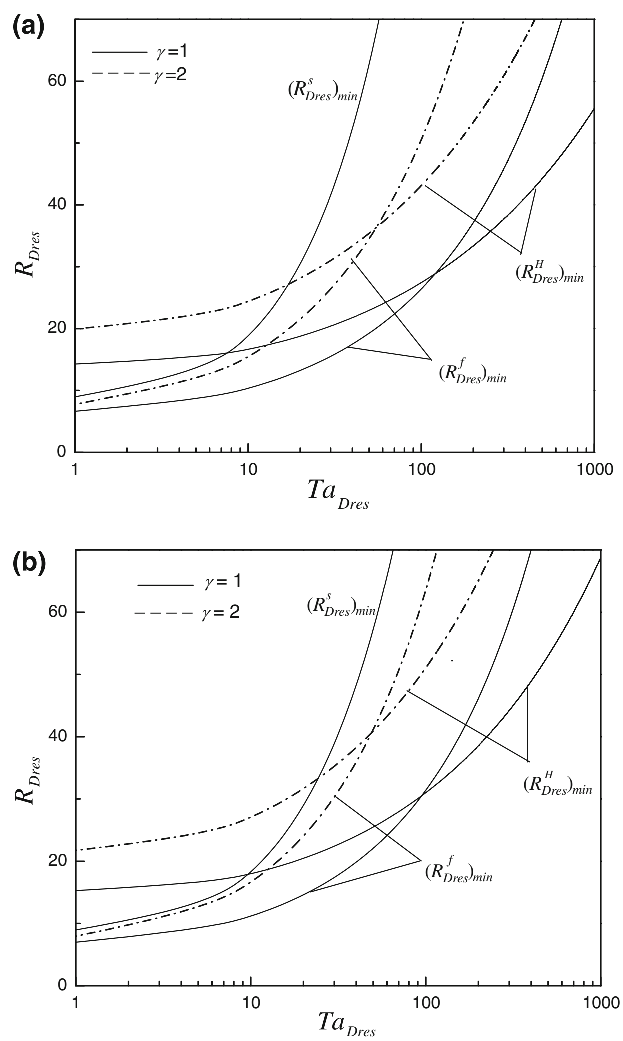

Fig. 6 Variation of $\left(R^s_{Dres}\right)_{\min}$, $\left(R^H_{Dres}\right)_{\min}$ and $\left(R^f_{Dres}\right)_{\min}$ as a function of Ta_{Dres} for **a** $\Lambda = 0.01$ and **b** $\Lambda = 0.03$ with $M = 1.25$

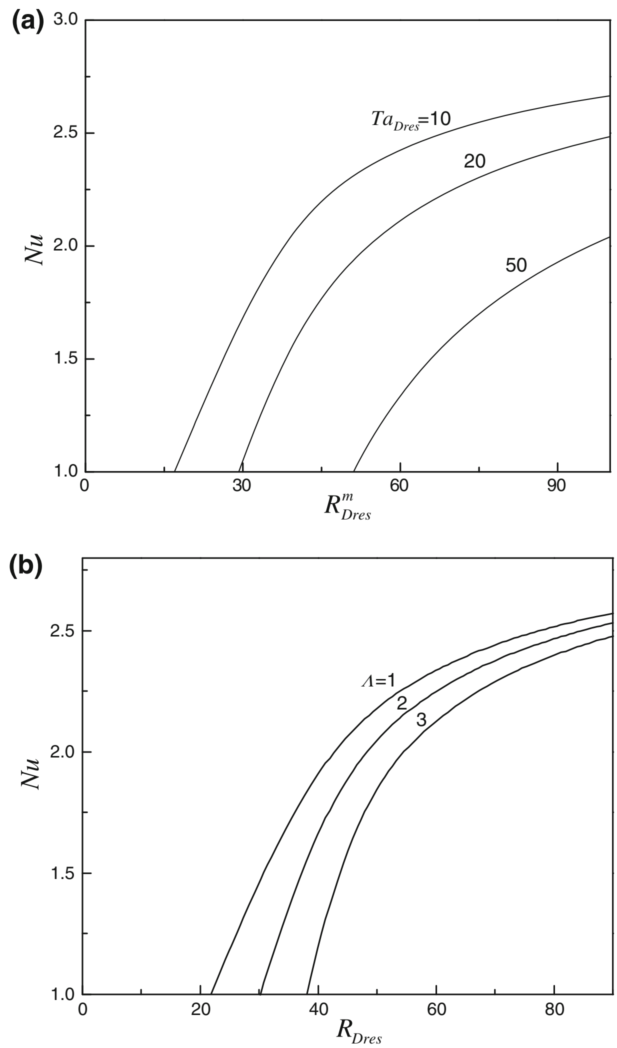

Fig. 7 *Nu* Vs R^s_{Dres} for different values of **a** Ta_{Dres} with $\Lambda = 0.1$ and **b** Λ with $Ta_{Dres} = 10$, when $\gamma = 10$ and $M = 1.25$

When $Ta_{Dres} = 0$, from Eq. (53) it is observed that R^s_{Dres} is an increasing function of Λ indicating the effect of increasing couple-stress parameter is to delay the onset of steady convection. In other words, the presence of couple-stresses is to stabilize the fluid motion against convection in the absence of any rotational effects. When $Ta_{Dres} \neq 0$ (i.e., in the presence of rotational effects), however, interestingly it can be seen that the right-hand side of Eq. (53) may become either negative or positive depending on the parametric values. That is to say, an increase in the value of Λ might lead to instability of a rotating *rigid* porous layer; result of contrast noticed when compared to a non-rotating case. Such a behavior is not noticed in the case of R^H_{Dres} and R^f_{Dres}, where these two Rayleigh numbers are found to be monotonically increasing functions of Λ.

The destabilization due to couple-stress parameter on the steady onset in the presence of rotational effects has been distinctly exhibited graphically in Fig. 3. This figure depicts the curves of $\left(R^s_{Dres}\right)_{\min}$ (minimum value of R^s_{Dres} obtained with respect to the wave number) as a function of Λ for different values of $Ta_{Dres} = 0$, 20, 30 and 40. As observed, $\left(R^s_{Dres}\right)_{\min}$ passes through a minimum with increasing Λ for different values of Ta_{Dres} considered except when $Ta_{Dres} = 0$ in which case $\left(R^s_{Dres}\right)_{\min}$ increases monotonically with Λ. The numerically calculated double minimum of R^s_{Dres} with respect to a and Λ for a fixed value of Ta_{Dres} is denoted by $\left(R^s_{Dres}\right)^c_{\min}$, and the corresponding critical value of a and Λ is denoted by a^c and Λ^c, respectively. The numerically computed values of $\left(R^s_{Dres}\right)^c_{\min}$ for different values of Ta_{Dres} are tabulated in Table 2. From the Table 2, we note that increase in Ta_{Dres} is to increase $\left(R^s_{Dres}\right)^c_{\min}$ and Λ^c, whereas a^c remains the same.

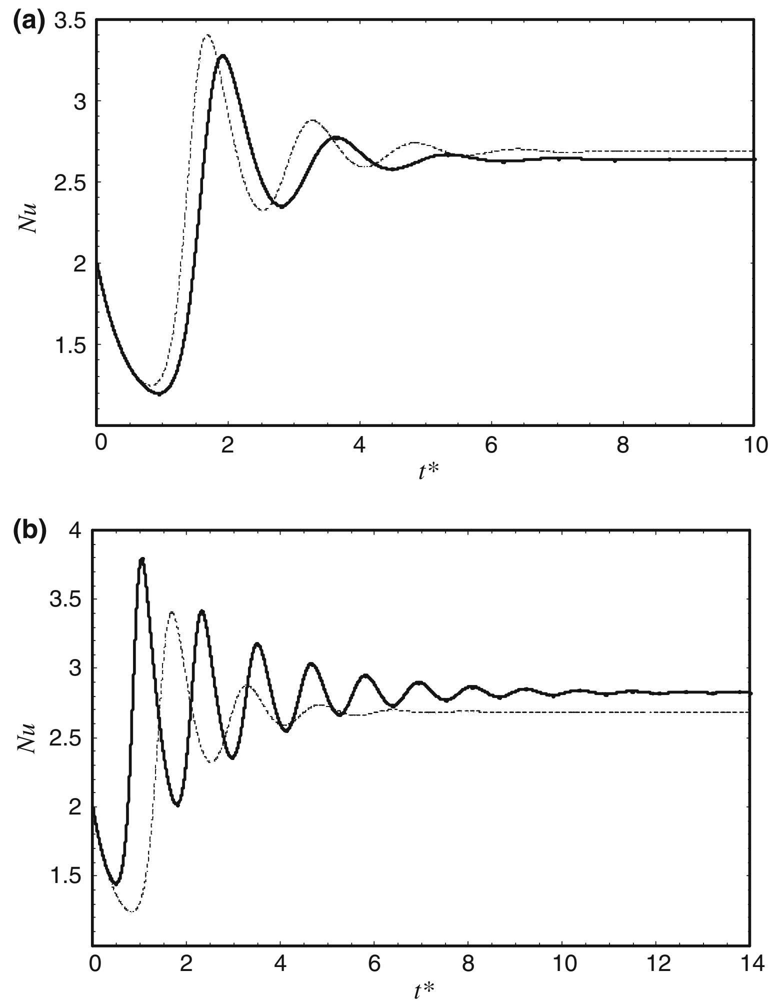

Fig. 8 Variation of *Nu* with time for $M = 1.25$, $Pr_D = 10$, $R_D^s = 9 \times 10^3$ for **a** $Ta_{D_{vphantom0_0}} = 50$ (dotted line), $Ta_D = 300$ (dashed line) with $\Lambda = 2$ and **b** $\Lambda = 1$ (dashed line) and $\Lambda = 2$ (dotted line) with $Ta_D = 50$

Table 2 Values of $\left(R_{Dres}^s\right)_{\min}^c$, a^c and Λ^c for various values of Ta_{Dres}

Ta_{Dres}	$\left(R_{Dres}^s\right)_{\min}^c$	a^c	Λ^c
10	16.432	2.0	0.275
20	23.238	2.0	0.527
30	28.461	2.0	0.721
40	32.863	2.0	0.884
50	36.742	2.0	1.027

To this effect, an analytic expression for Λ^c is obtained from Eq. (53) in the form

$$\Lambda^c = \frac{\sqrt{Ta_{Dres}}}{3\sqrt{3}} - \frac{1}{3} \tag{54}$$

and it is seen that Λ^c increases with an increase in the value of Ta_{Dres}.

The occurrence of minimum value of oscillatory Darcy–Rayleigh number R_{Dres}^H with respect to the wave number are, respectively, denoted by $\left(R_{Dres}^H\right)_{\min}$ and $a_{\min}^H$. The variation of $\left(R_{Dres}^H\right)_{\min}$ and $a_{\min}^H$ as a function of γ for different values of Ta_{Dres} is presented in Fig. 4a, b respectively for two values of $\Lambda = 0$ and 0.03 by fixing $M = 1.25$. The curves which are shown in these figures end at the point where no more values consistent with $\omega_{res}^2 > 0$ exist and it can be seen that the ending point of the figures increases with an increase in the value of Ta_{Dres} and also when the couple-stress effect is not present. Further, increase in Ta_{Dres} and Λ is to delay the onset of oscillatory convection as noted earlier (see Fig. 4a). Although increase in Ta_{Dres} is to contract the size of convection cells, opposite is the case with an increase in Λ (see Fig. 4b).

Substituting $a^H_{\min}$, which minimizes R^H_{Dres}, in Eq. (28) yields the corresponding minimum value of the frequency, which is presented in terms of $\left(\omega^2_{res}\right)_{\min}$. Figure 5 depicts the variation of $\left(\omega^2_{res}\right)_{\min}$ with logγ for different values of Ta_{Dres} and for two values of $\Lambda = 0$ and 0.03 when $M = 1.25$. A marked increase in the frequency with increasing Taylor number is noticed from the figure, while large values of the frequency are particularly related to small values of γ, and they decay as γ increases. Also, the presence of couple-stresses leads to only marginal increase in $\left(\omega^2_{res}\right)_{\min}$ up to $\gamma \leq 1$ and an opposite trend could be seen with further increase in γ.

The variation of $\left(R^s_{Dres}\right)_{\min}$, $\left(R^H_{Dres}\right)_{\min}$ and $(R^f_{Dres})_{\min}$ as a function of Ta_{Dres} is shown in Fig. 6a, b for Λ= 0.01 and 0.04, respectively, with $M = 1.25$ in order to know the preferred type of instability. From these two figures, it is seen that up to a certain range of Ta_{Dres}, depending on the value of γ and Λ, sub-critical instability is possible and exceeding this range of Ta_{Dres} oscillatory instability is preferred. Moreover, the range of Ta_{Dres}, up to which sub-critical instability is preferred, is found to increase marginally with the decrease in the value of γ and Λ.

The heat transport calculated in terms of Nusselt number *Nu*, as a function of R^s_{Dres} is shown in Fig. 7a, b for different values of Ta_{Dres} and Λ, respectively, when $\gamma = 10$ and $M = 1.25$. From these figures it is evident that increase in the value Ta_{Dres} and Λ is to decrease the quantity of heat transfer due to their stabilizing effect on the system. The transient behavior of Nusselt number is shown in Fig. 8a, b as a function of time t^* by solving the nonlinear system of Eq. (13a–e) using the Runge–Kutta–Gill method with appropriate initial conditions. From the figures it is seen that although the Nusselt number oscillates initially with time, it reaches a steady state as time progresses. Further, increase in the value of Ta_{Dres} (see Fig. 8a) and Λ (see Fig. 8b) is to dampen the amplitude of the oscillations of heat flux and hence to decrease the value of Nusselt number.

8 Conclusions

The linear and weakly nonlinear thermal convection in a rotating couple-stress fluid-saturated *rigid* porous layer are investigated in depth. It is found that the domain of the Prandtl number for the occurrence of oscillatory convection depends on the value of heat capacity ratio *M* and couple-stress parameter Λ_c. It is shown that Hopf bifurcation is possible in the presence of Coriolis force due to rotation. It is established that Hopf bifurcation is possible always at a lower value of the Darcy–Rayleigh number at which simple/direct bifurcation occurs. The effect of increase in Taylor number is to reinforce stability on the fluid motion against convection. In the absence of rotational effects, increase in the value of Λ_c is to delay the onset of convection. To the contrary, it is found that the presence of couple-stresses shows some destabilization initially on the steady onset when the rotational effects are present. The range of values of Λ_c up to which the system gets destabilized increases as the strength of rotation increases. Nonetheless, increasing Λ_c is to delay the onset of oscillatory and finite amplitude steady convection. The nonlinear autonomous ordinary differential equations are solved numerically for the unsteady case and analytically for the steady case. It is observed that sub-critical finite amplitude steady motions occur depending on the choice of physical parameters but at higher rotation rates oscillatory convection is the preferred mode of instability. Further, increase in the value of Taylor number and the couple-stress parameter is to dampen the oscillations of Nusselt number and thereby to decrease the heat transfer.

Acknowledgments This work was supported by the UGC-Centre for Advanced Studies in Fluid Mechanics. One of the authors (SSK) would like to thank the Director, Principal and Management of Siddaganga Institute of Technology, Tumkur for their encouragement. The authors wish to thank the reviewer for useful comments that helped in improving the paper.

References

1. Kakac, S., Kilkis, B., Kulacki, F.A., Auric, F.: Convective Heat and Mass Transfer in Porous Media. Kluwer, Dordrecht (1991)
2. Kaviany, M.: Principles of Heat Transfer in Porous Media. 2nd edn. Springer, New York (1991)
3. Bejan, A.: Convection Heat Transfer. 2nd edn. Wiley, New York (1995)
4. Vafai, K.: Handbook of Porous Media. Marcel Dekker, New York (2000)

5. Vafai, K.: Handbook of Porous Media. 2nd edn. Taylor and Francis (CRC), Boca Raton (2005)
6. Nield, D.A., Bejan, A.: Convection in Porous Media. 3rd edn. Springer, New York (2006)
7. Chandrasekhar, S.: Hydrodynamic and Hydromagnetic Stability. Oxford University Press, London (1961)
8. Galdi, G.P., Straughan, B.A.: Nonlinear analysis of the stabilizing effect of rotation in the Benard problem. Proc. R. Soc. Lond. A **402**, 257 (1985)
9. Kloosterziel, R.C., Carnevale, G.F.: Closed form linear stability conditions for rotating Rayleigh-Benard convection with rigid stress- free upper and lower boundaries. J. Fluid Mech. **480**, 25 (2003)
10. Friedrich, R., Rudraiah, N.: Numerical study of large amplitude convection in a rotating fluid-saturated porous layer. In: Proceedings of IV GAMM Conference on Numerical methods in Fluid Mechanics, p. 7. Viewieg, Paris (1981)
11. Palm, E., Tyvand, P.A.: Thermal convection in a rotating porous layer. J. Appl. Math. Phys. (ZAMP) **35**, 122 (1984)
12. Qin, Y., Kaloni, P.N.: Nonlinear stability problem of a rotating porous layer. Q. J. Appl. Math. **LIII**, 129 (1995)
13. Vadasz, P.: Coriolis effect on gravity-driven convection in a rotating porous layer heated from below. J. Fluid Mech. **276**, 351 (1998)
14. Vadasz, P.: Flow and thermal convection in rotating porous media. In: Vafai, K. (ed.) Handbook of Porous Media, p. 395. Marcel Dekker, Inc, New York (2000)
15. Straughan, B.: A sharp nonlinear stability threshold in rotating porous convection. Proc. R. Soc. Lond. A **457**, 87 (2001)
16. Govender, S.: Coriolis effect on the linear stability of convection in porous layer placed far away from the axis of rotation. Transp. Porous Med. **51**, 315 (2003)
17. Straughan, B.: Global nonlinear stability in porous convection with a thermal non-equilibrium model. Proc. R. Soc. Lond. A **462**, 409 (2006)
18. Malashetty, M.S., Mahantesh, S., Sridhar, K.: Thermal convection in a rotating porous layer using a thermal nonequilibrium model. Phys. Fluids **19**(5), 1 (2007)
19. Shivakumara, I.S., Savitha, M.N., Krishna, B.C., Devaraju, N.: Bifurcation analysis for thermal convection in a rotating porous layer. Meccanica **44**, 225 (2009)
20. Shenoy, A.V.: Non-Newtonian Fluid Heat Transfer in Porous Media, Advances in Heat Transfer. Academic Press, San Diego, CA (1994)
21. Eringen, A.C.: Theory of micropolar fluids. J. Math. Mech. **16**, 1 (1966)
22. Stokes, V.K.: Couple-stresses in fluids. Phys. Fluids **91**, 709 (1966)
23. Goel, A.K., Agarawal, S.C.: Hydromagnetic stability of an unbounded couple-stress binary fluid mixture having vertical temperature and concentration gradients with rotation. Indian J. Appl. Math. **30**(10), 991 (1999)
24. Sunil, Sharma, R.C., Mohinder, P.: On couple-stress fluid heated from below in porous medium in the presence of rotation. App. Mech. Engg. **5**(4), 883 (2000)
25. Sunil, Sharma, R.C., Mohinder, P.: On a couple-stress fluid heated from below in porous medium in the presence of magnetic field and rotation. J. Porous Media **5**(2), 149 (2002)
26. Sunil, Sharma, R.C., Rajender Singh, C.: Effect of suspended particles on couple-stress fluid heated and soluted from below in porous medium. J. Porous Media **7**(1), 9 (2004)
27. Malashetty, M.S., Gaikwad, S.N., Mahantesh, S.: An analytical study of linear and non-linear double diffusive convection with Soret effect in couple-stress liquids. Int. J. Therm. Sci. **45**, 897 (2006)
28. Gaikwad, S.N., Malashetty, M.S., Rama Prasad, K.: An analytical study of linear and non-linear double diffusive convection with Soret and Dufour effects in couple-stress liquids. Int. J. Nonlinear Mech. **42**(7), 903 (2007)
29. Malashetty, M.S., Shivakumara, I.S., Sridhar, K.: The onset of convection in a couple-stress fluid-saturated porous layer using a thermal non-equilibrium model. Phys. Lett. A **373**, 781 (2009)
30. Shivakumara, I.S.: Onset of convection in a couple-stress fluid-saturated porous medium: effects of non-uniform temperature gradients. Arch. Appl. Mech. (2009) doi:10.1007/s00419-009-0347-5
31. Hubbert, M.K.: Darcy's law and the field equations of the flow of underground fluids. Trans. Am. Inst. Min. Met. Eng. **207**, 222 (1956)
32. De wiest, R.J.M.: Geohydrology. Wiley, New York (1965)
33. Veronis, G.: Motions at subcritical values of the Rayleigh number in a rotating fluid. J. Fluid Mech. **24**, 545 (1966)
34. Moroz, M.: Interacting steady and oscillatory rolls in triple convection. Geophys. Asrophys. Fluid Dyn. **41**, 313 (1988)